Supplementary Materials

In this supporting file, there were 2 texts, 2 table and 6 figures.

Content in this SI files

Text S1 The detail procedure of •OH quantitative experiment
Text S2 The detail procedure of $•O_2^-$ quantitative experiment
Table S1 Structural properties of NPCR catalysts
Table S2 Comparison of different metal-free catalysts performance on OA degradation.
Figure S1 The chemical structure of D412
Figure S2 The images of (a) NPCR-600, (b) NPCR-700, (c) NPCR-800 and (d) NPCR-900.
Figure S3 Linear fit between graphitic N (a), pyrrolic N (b), pyridinc N (c), C-O-P (d), C-P-O (e) and I_D/I_G value.
Figure S4 The zeta potential of NPCR-800.
Figure S5 Degradation of OA in O_3 and NPCR-800/O_3 systems under near neutral condition. Conditions: [OA] = 150 mg/L, [Catalyst] = 0.5 g/L, gaseous [O_3] = 60 mg/L, O_3 flow rate = 100 ml/min, initial pH (without adjustment) = 2.8.
Figure S6 Linear fit between C-O-P (a), C-P-O (b) and reaction rate constants k_{obs}.

Text S1 The detail procedure of •OH quantitative experiment. In this study, •OH quantitative experiment was conducted as described by Jin et. al [1]**.** Briefly, 5 mg coumarin was added to 0.5 L ozone water at a concentration of 15 mg/L, followed by adding 0.25 g of NPCR-800. 5 ml of water samples were obtained from the reactor and filtered by a 0.45 μm PTFE filter at given time intervals. 0.5 ml of sodium hyposulfite solution was added to each sample for quenching the ozonation/catalytic ozonation. The standard curve was constructed with 7-hydroxycoumarin, with an emission wavelength of 455 nm, an excitation wavelength of 332 nm, and a slit width of 5 nm.

Text S2 The detail procedure of $•O_2^-$ quantitative experiment. First, the standard curve of UV absorbance of NBT (Nitrotetrazolium blue chloride) at 340 nm was constructed. Before $•O_2^-$ quantitative experiment, the NBT adsorption experiment was conducted. In detail, 0.25 g NPCR-800 was added to 0.5 L NBT solution with a concentration of 100 mg/L. 5 ml of water samples were obtained from the reactor and filtered by a 0.45 μm PTFE filter at given time intervals. then the UV absorbance of samples at 340 nm was determined. $•O_2^-$ quantitative experiment was performed in similar procedures. Briefly, 50 mg NBT was added to 0.5 L ozone water with a concentration of 15 mg/l, and then 0.25 g NPCR was introduced. Other steps of $•O_2^-$ quantitative experiment were as same as the that of NBT adsorption experiment. The

residual NBT in the solution was calculated according to the standard curve, and the production of $\bullet O_2^-$ could be obtained by calculation through the amount of NBT consumed, which as described by Goto et al. [2]. The NBT adsorbed on NPCR was determined, which was deducted as a blank from the NBT consumed at each given interval.

Table S1 Structural properties of NPCR catalysts

Sample	S_{BET} (m^2/g)
NPCR-600	284.7
NPCR-700	397.1
NPCR-800	557.2

Table S2 Comparison of different metal-free catalysts performance on OA degradation.

Metal-free catalysts	Reaction constant (min^{-1})	OA concentration (mg/L)	O_3 consumption to degrade per unit mass of OA (mg O_3/mg OA)	Reference
Active reduced graphene oxides	0.1	50	6	[3]
N-doped spongy carbon	0.109 ± 0.008	100	0.6	[4]
N-doped nanocarbons	0.076	50	4.5	[5]
Metal-free graphitic framework with built-in nanotubes	>0.128	50	2	[6]
NPCR-800	0.062	150	3.5	This work

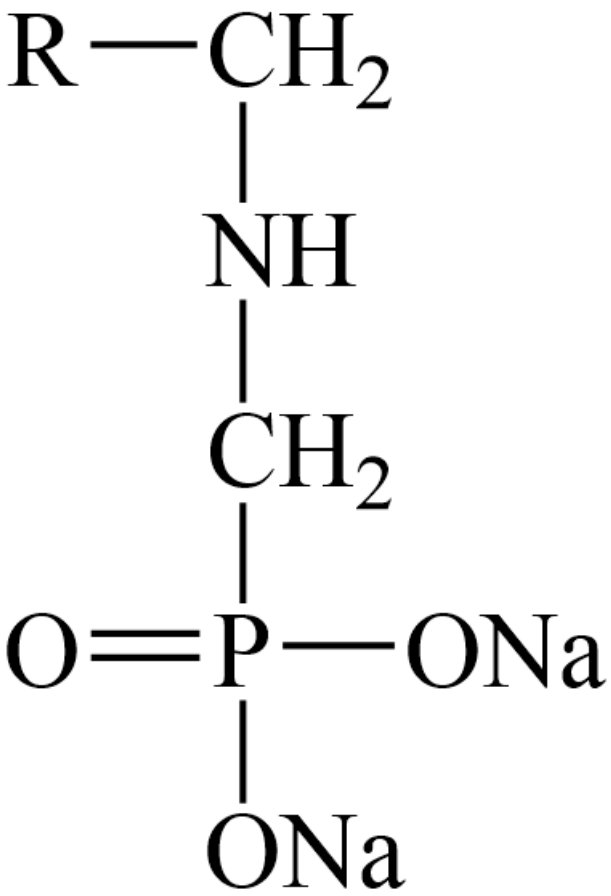


Figure S1 The chemical structure of D412

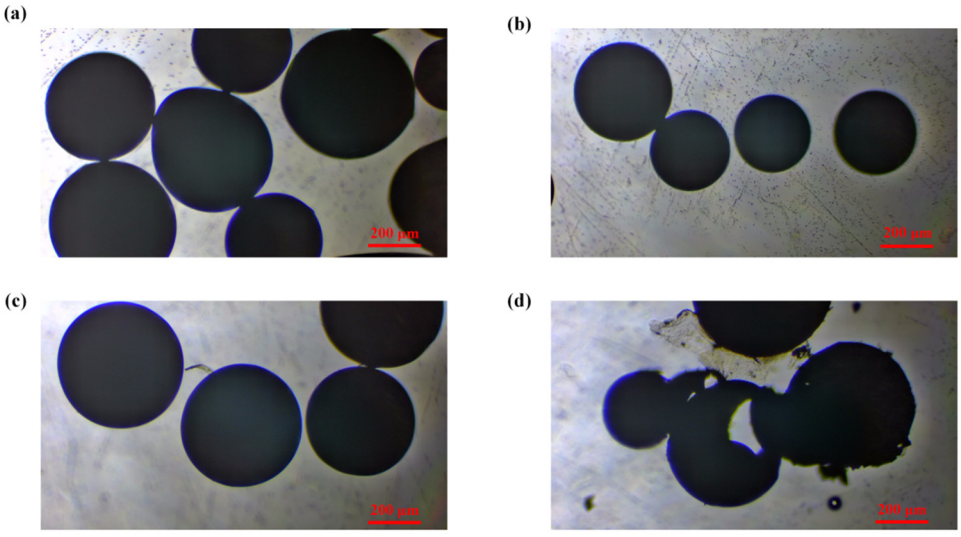


Figure S2 The images of (a) NPCR-600, (b) NPCR-700, (c) NPCR-800 and (d) NPCR-900.

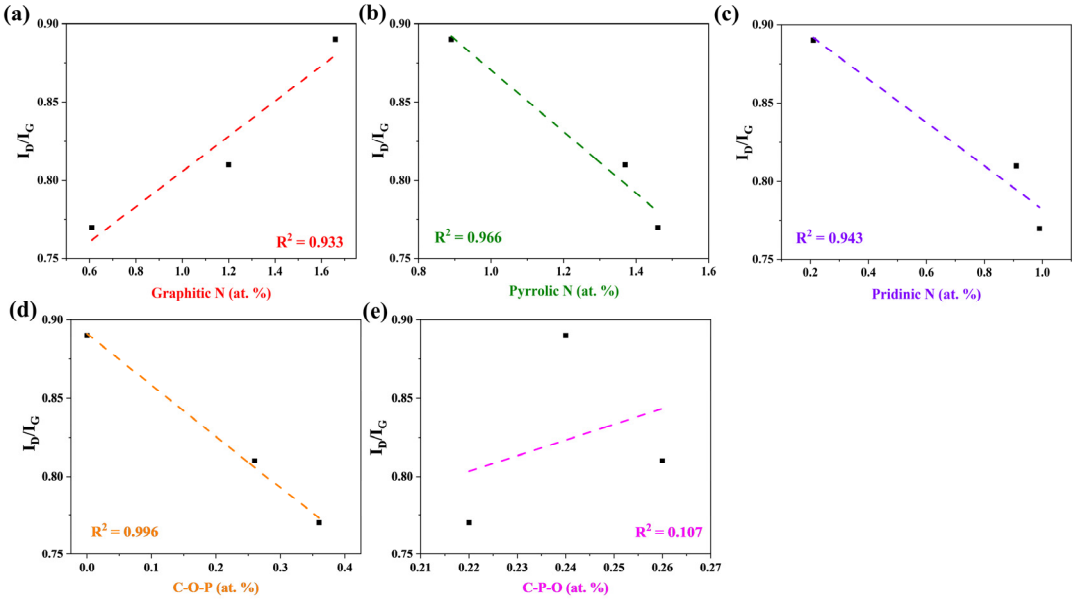


Figure S3 Linear fit between graphitic N (a), pyrrolic N (b), pyridinc N (c), C-O-P (d), C-P-O (e) and I_D/I_G value.

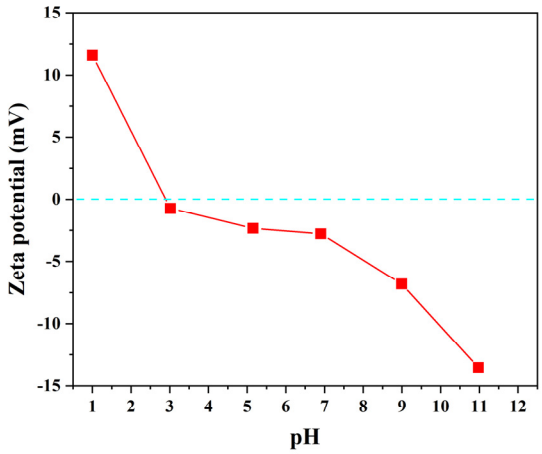


Figure S4 The zeta potential of NPCR-800.

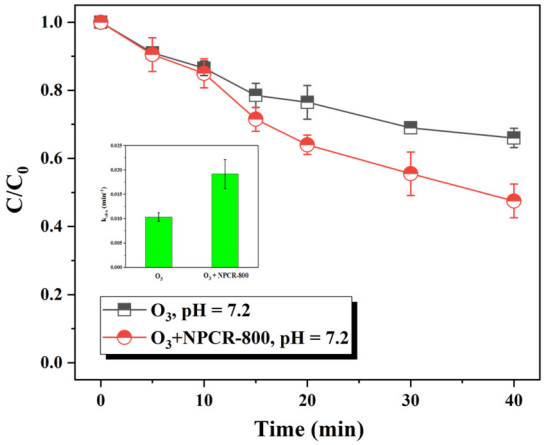


Figure S5 Degradation of OA in O_3 and NPCR-800/O_3 systems under near neutral condition. Conditions: [OA] = 150 mg/L, [Catalyst] = 0.5 g/L, gaseous [O_3] = 60 mg/L, O_3 flow rate = 100 ml/min, initial pH (without adjustment) = 2.8.

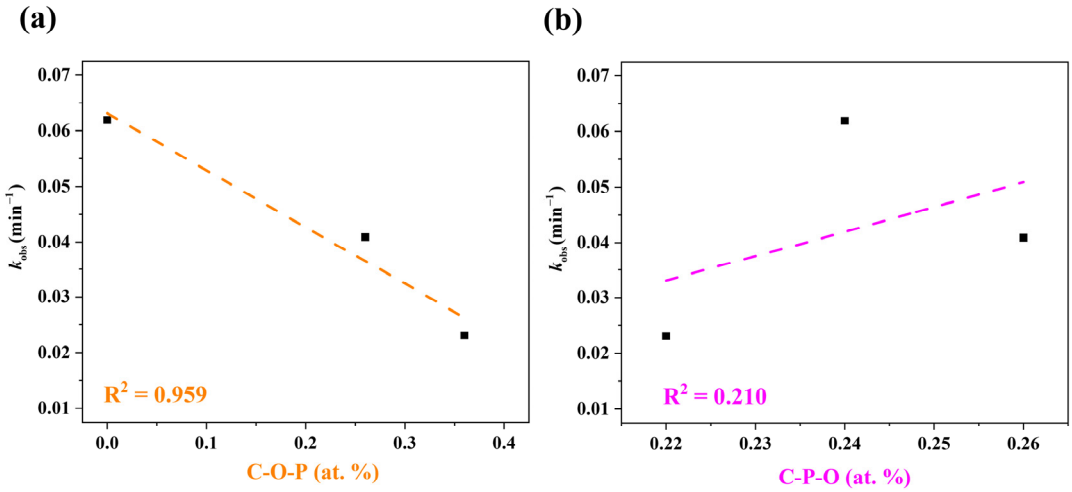


Figure S6 Linear fit between C-O-P (a), C-P-O (b) and reaction rate constants k_{obs}.

References

[1] X. Jin; Z. Wu; C. Wan; J. Zuo; Y. Zhou; X. Tian; P. Wang; C. Sun; C. Wu Magnetic nano-size normal spinel-ZnFe2O4 and inverse spinel-$MnFe_2O_4$ for catalytic ozonation: Performance and mechanism. *Sep. Purif. Technol.* **2023**, *313*.

[2] H. Goto; Y. Hanada; T. Ohno; M. Matsumura Quantitative analysis of superoxide ion and hydrogen peroxide produced from molecular oxygen on photoirradiated TiO_2 particles. *J.*

Catal. **2004**, *225*, 223-229.
[3] Y. Wang; H. Cao; L. Chen; C. Chen; X. Duan; Y. Xie; W. Song; H. Sun; S. Wang Tailored synthesis of active reduced graphene oxides from waste graphite: Structural defects and pollutant-dependent reactive radicals in aqueous organics decontamination. *Appl. Catal., B* **2018**, *229*, 71-80.
[4] J. Chen; C. Yang; T. Wu; J. Wang; L. Yang; W. Sun; W. Li; A. Wang; S. Lv Metal-free N-doped spongy carbon recycled from waste MOF for enhanced catalytic ozonation: Mechanistic insights and practical applications. *J. Water Process Eng.* **2023**, *55*.
[5] Y. Wang; L. Chen; C. Chen; J. Xi; H. Cao; X. Duan; Y. Xie; W. Song; S. Wang Occurrence of both hydroxyl radical and surface oxidation pathways in N-doped layered nanocarbons for aqueous catalytic ozonation. *Appl. Catal., B* **2019**, *254*, 283-291.
[6] Y. Wang; J. Xi; X. Duan; W. Lv; H. Cao; C. Chen; Z. Guo; Y. Xie; S. Wang The duet of surface and radical-based carbocatalysis for oxidative destructions of aqueous contaminants over built-in nanotubes of graphite. *J. Hazard. Mater.* **2020**, *384*.